HHS Public Access

Author manuscript

Cardiovasc Intervent Radiol. Author manuscript; available in PMC 2021 January 01.

Published in final edited form as:

Cardiovasc Intervent Radiol. 2020 January ; 43(1): 84–93. doi:10.1007/s00270-019-02300-y.

Peri-Tumoral Metallic Implants Reduces the Efficacy of Irreversible Electroporation for the Ablation of Colorectal Liver Metastases

Francois H. Cornelis, MD, PhD[1,2], **Helena Cindrič, MsC**[3], **Bor Kos, PhD**[3], **Masashi Fujimori, MD**[1], **Elena N. Petre, MD**[1], **Damijan Miklavčič, PhD**[3], **Stephen B. Solomon, MD**[1,4], **Govindarajan Srimathveeravalli, PhD**[4,5]

[1]Department of Radiology, Memorial Sloan-Kettering Cancer Center. 1275 York Avenue. New York. NY 10065. USA

[2]Sorbonne Université, ISCD, Tenon Hospital. 4 rue de la Chine. 75020 Paris. France

[3]University of Ljubljana, Faculty of Electrical Engineering, Tržaška 25, SI 1000, Ljubljana, Slovenia

[4]Dept. of Mechanical and Industrial Engineering, University of Massachusetts, Amherst, MA 01003. USA

[5]Institute for Applied Life Sciences, University of Massachusetts, Amherst, MA 01003. USA

Abstract

Purpose: To evaluate the effect of peri-tumoral metallic implants (MI) on the safety and efficacy of percutaneous irreversible electroporation (IRE) of colorectal liver metastasis (CRLM).

Materials and Methods: In this retrospective study, 25 patients (12 women, 13 men; MI: 13, No MI: 12) were treated for 29 CRLM. Patient characteristics, tumor location and size, treatment parameters and the presence of MI were evaluated as determinants of local tumor progression (LTP) with the competing risks model (uni- and multivariate analyses). Patient specific computer

Corresponding author: Govindarajan Srimathveeravalli, N573, Life Sciences Lab, 240 Thatcher Way, Amherst, MA, 01003, 413-545-6491, govind@umass.edu.

Conflict of Interest: The authors report no relevant conflict of interest related to the work presented here. S.B.S is a consultant to BTG, Johnson & Johnson, XACT, Adegro and Medtronic. S.B.S is a consultant to BTG, Johnson & Johnson, XACT, Adgero, Innobaltive, and Medtronic. S.B.S has funding support from GE Healthcare, Ethicon, Elesta and Angiodynamics, and holds stock in Aperture Medical.

Compliance with Ethical Standards

Ethical Approval: All procedures were performed in accordance with the ethical standards of the institutional or national research committee, and with the Helsinki declaration and its later amendments or comparable ethical standards. This is a retrospective study; informed formal consent is not required.

Informed Consent: For this type of study informed consent is not required.

Consent for Publication: For this type of study consent for publication is not required.

models were created to examine the effect of the MI on the electric field used to induce IRE, probability of cell kill and potential thermal effects.

Results: Patients had a median follow-up of 25 months, during which no IRE related major complications were reported. Univariate analysis showed that tumor size (> 2cm), probe spacing (> 20 mm), and the presence of MI ($p < 0.05$) were significant predictors of time to LTP, but only the latter was found to be an independent predictor on multivariate analysis (sub-hazard ratio = 6.5, [95% CI: 1.99, 21.4], $p = 0.002$). Absence of peri-tumoral MI was associated with higher progression free survival at 12 months (92.3% [56.6, 98.9] vs 12.5% [2.1, 32.8]). Computer simulations indicated significant distortions and reduction of electric field strength near MI, which could have contributed to under-treatment of the tumor.

Conclusions: Peri-tumoral MI increases the risk of treatment failure following IRE of CRLM.

Keywords

Liver; Colorectal Metastasis; Irreversible electroporation; Survival; Local Tumor Progression; Computer Simulations

Introduction

Irreversible electroporation (IRE) has been evaluated for the ablation of primary (1–3) and metastatic tumors (4,5) in the liver that cannot be treated with thermal ablation because of safety or efficacy concerns. The largely non-thermal tumor killing effect of IRE has allowed its use for the treatment of tumors abutting the bile duct and large blood vessels in the liver (6,7). Early studies report efficacious local control of colorectal liver metastases (CRLM) using IRE (4,5), and tumor diameter greater than 3 cm has been reported to be the only independent risk factor for local tumor progression following ablation (3). Patients selected to undergo ablation of their CRLM may have undergone prior treatment such as surgical resection, and can therefore have surgical clips, biliary stents or other metallic implants in the vicinity (< 1cm) of the tumor to be treated. Metallic implants (MI) have substantially greater electrical conductivity than the tumor or healthy liver, and may influence the distribution and strength of the electric field applied during IRE (8,9). The presence of MI can also create pockets of high current density, leading to undesirable effects such as electrical arcing and localized heating (8). While the presence of large MI such as stents are a contraindication to the application of IRE as per manufacturer IFU, the presence of small MI such as surgical clips at the site of ablative treatment is a common clinical scenario in the management of unresectable liver malignancies. Therefore, the objective of this study was to understand the effect of metallic implants on the safety and efficacy of percutaneous IRE of CRLM. Our hypothesis was that MI will reduce the efficacy of CRLM ablation with IRE, and that patient specific computer models can be used as a novel tool to identify the mechanism by which MI affect IRE outcomes.

Material and Methods

Patient Selection and Eligibility Criteria

Retrospective review of all patients who underwent IRE of their CRLMs at our institution, a tertiary cancer center, between 2011 and 2015 was performed under a HIPPA compliant, IRB approved protocol.

Treatment

The decision to use IRE to treat patients' CRLMs was entirely at the IR physician's discretion and was driven by the tumor's proximity to large (> 3 mm) blood vessels or major bile ducts, where thermal ablation would increase the risk of complications or LTP. All procedures were performed while the patients were under general anesthesia and deep muscle relaxation, and electric pulse delivery was synchronized to the patient's electrocardiogram. All treatments were performed with the NanoKnife system (Angiodynamics, NY, USA), using CT guidance for electrode placement by two interventional radiologists with more than 15 years of experience performing percutaneous ablation and 7 years of experience performing IRE in patients. Electrode geometry and treatment parameters were selected with the intent to treat the tumor while achieving a minimum of 5 mm ablation margin. Triphasic CT was performed immediately after ablation to evaluate technical success of the ablation. Complete coverage of the tumor and a 5mm ablation margin with a non-enhancing region on immediate post-treatment CT imaging was defined as the ablation endpoint. All patients included in this study received systemic chemotherapy as per standard of care for their disease status during the follow-up period.

Imaging Follow-up and Local Tumor Progression

Triphasic liver CT imaging was performed within 4-8 weeks after IRE ablation and every 2-4 months thereafter through the follow-up period. IRE success was defined as the absence of irregular peripheral or nodular enhancement within 1 cm of the ablated area at the first imaging follow-up. Imaging appearance indicating otherwise was considered treatment failure with residual tumor at the first imaging follow-up (4-8 weeks) (26). Evidence of new abnormal tumor tissue (i.e. tumor recurrence) within 1 cm from the ablation zone observed on contrast-enhanced CT images obtained after the first imaging follow-up, and confirmed by review was considered local tumor progression (LTP). This approach is consistent with the guidelines on reporting of tumor ablation (26,10). Positron emission tomography (PET) was performed at 6- and 12-months following ablation and presence of increased SUV uptake was considered positive evidence of local tumor progression. Procedure-related complications and side effects were noted and classified on the basis of criteria proposed by the Society of Interventional Radiology (11), CIRSE complication classifications (32) and the National Cancer Institute Common Terminology Criteria Adverse Events (CTCAE, version 4.0). The operating interventional radiology physicians retrospectively reviewed imaging assessments. Evidence of tumor recurrence up to 1 cm from the ablation zone seen on contrast-enhanced CT images and confirmed by the review was considered LTP.

Numerical calculations

A subset of all patients included in the study, four with MI in the vicinity of ablation zone (up to 1 cm from the tumor and or the electrodes) and four without, were selected for evaluation of treatment delivery with computer simulations. The number of ablation probes used for the treatment (≤ 4) and the availability of complete intraprocedural treatment parameters data was used to select the sub-set of patients for evaluation with computer simulations. The selected datasets and corresponding treatment parameters (voltage, electrode spacing and exposure, and the number of pulses) were exported to Visifield (12). Visifield is a web-based tool for visualizing in vivo distribution of electric fields during electroporation-based treatments. Patients' pre-procedural CT images were manually segmented by an experienced radiologist (M.F.) to demarcate the tumor, liver parenchyma, major anatomic landmarks such as blood vessels, and to define positions and orientations of any metallic surgical clips in the treatment vicinity (Fig. 1A). Intra-procedural CT images were registered to preprocedural images and used to determine the positions of IRE electrodes during treatment (Fig. 1B). A 3D numerical model was built for each patient and tumor (Fig. 1C). Electric field distribution was computed using a nonlinear model of electric field dependent tissue conductivity. Tissue heating was taken into account by solving the Pennes' bioheat equation. Electrical and thermal properties of the modelled tissues (e.g. liver, blood, and tumor density, thermal capacity and conductivity, etc.) were compiled from the literature in previous work (13). The electric field was computed for each electrode pair present in the treatments. The total extent of the ablation zone was evaluated by combining the maximal computed electric field in situ from all electrode pairs (14), and regions that may have experienced insufficient field strength for complete ablation were identified. Probability of cell death due to irreversible electroporation was calculated using a statistical Peleg-Fermi model, which also takes into account the number of applied electrical pulses(15). Model parameters were adjusted to best describe the properties of liver tissue during IRE treatment. The probability of cell death due to thermal damage was calculated using the Arrhenius equation (16). The volume of the tumor experiencing electric field greater than the critical threshold, where the probability of cell death due to IRE or thermal damage was > 0.9 were calculated as the percentage of the pre-treatment tumor volume.

Statistical Analysis

Median follow-up time was determined based on patients who were alive at the end of the review period. Survival rates were calculated by using the Kaplan-Meier method and were stratified for gender, tumor location, tumor size (> 2 cm), number of ablation probes (> 3), treatment parameters (probe spacing > 2 cm, treatment voltage < 2500 V, pulse length < 100 microseconds, and the number of pulses applied < 90), and the presence of metallic surgical clips within 1 cm from the tumor margin. Variables that showed statistical significance at univariate analysis were subsequently analyzed with a multivariate model. As patient death may occur prior to evidence of LTP on imaging, LTP predictors were adjusted for competing factors for death using the Fine-Gray competing risks regression model (17). This analysis enabled us to identify specific factors contributing to the risk of LTP by modeling sub-distribution functions of LTP, death without LTP, along with the associated hazard rates (HR) and the sub-hazard ratio (sHR). Results of this analysis is shown along with the Kaplan-Meyer technique for comparison. Differences in electric field coverage, cell death

probability and thermal damage in simulation models within (clips vs. no clips) and between patients were assessed with a Mann-Whitney U test. Data were analyzed with a commercially available statistical software (Stata, version 12.0; Stata, College Station, Texas).

Results

The study enrolled 25 consecutive patients who underwent IRE of 29 CRLMs. Amongst these patients, 13 had MI in the peri-tumoral region and 12 did not have MI. All patients completed follow-up and were included in the analysis. Patient and tumor characteristics, and treatment parameters used to perform IRE are detailed in Table 1 and Table 2 respectively.

Clincal Outcomes.

IRE treatment failure was observed in 13.8% of tumors (4/29) at the first postablation CECT scan (Fig. 2 A–F) performed 4-8 weeks following treatment, and all cases with residual tumor were patients with MI (Fig. 2 D–E). Subsequent tumor progression was observed in 58.6% of tumors (17/29) during the median follow up period of 25 months (Fig. 3 A–C) wherein all patients had MI. The cumulative survival without LTP was 48.3% [95% confidence interval [CI]: 29.5, 64.8] and 40.5% [22.6, 57.7] at the 12 and 24-month follow-up respectively. Univariate analysis suggested that tumor size >2 cm (p=0.003), probe spacing > 2 cm (p=0.018), and the presence of metallic clips within 1cm of ablation probes (p = 0.001) to be significant predictors of time to LTP. Gender of the patient (p = 0.997), the tumor location (p = 0.445), the number of probes used for the treatment (p = 0.252), treatment voltage < 2500 V (p = 0.582), pulse length < 100 microseconds (p = 0.830), or the number of pulses applied < 90 pulses (p=0.830) were not found to be determinants of LTP. On subsequent multivariate analysis only the presence of metallic clips (HR, 29.5; P = 0.002) was found to be an independent predictor of shorter time to LTP (Table 3). As patient death may have occurred before imaging evidence of LTP could be gathered, a competing analysis was performed. The resulting sHR of the presence of metallic clips as predictor of LTP was still significant (sHR: 6.5, 95% CI: 1.99, 21.4, P =0.002). Kaplan-Meier survival curve of LTP are displayed in Fig. 4A. In the absence of metallic clips in the vicinity of ablation, the progression free survival rate was 92.3% (56.6, 98.9) at 6-36 months. In presence of metallic clips, the progression free survival rate was 18.8% (4.6, 40.3) at 6 months, 12.5% (2.1, 32.8) at 12 months, and 0% after. Overall survival rate was 82.8% [63.4, 92.4] at 12 months, 61.3% [40.1, 76.5] at 24 months, and 26.8% [12, 44.2] at 36 months (Fig. 4B). Progression of disease was the cause of death in all patients, and assessed variables were not found to be predictors of overall survival, including tumor size of greater than 2 cm (HR=1.92; [0.78-4,7]; p = 0.154) and the presence of metallic clips (HR=2; [0.81-4,92]; p=0.132).

Treatment related complications of grade > 3 were not observed. Six complications with grade < 3 occurred following the procedures. This included pneumothoraxes (n=5, 4 requiring drainage), and 1 case of urinary retention. Complication related to injury of the liver, blood vessels of the liver, bile ducts, small bowel or duodenum were not observed.

Simulation Outcomes.

Ablation was considered technically successful if the electric field strength exceeded the threshold for IRE in the liver (500 V/cm) (31) and the probability of cell death was > 0.9 in the tumor and the margin (Fig. 1 D–F). In patients with MI, the electric field was computed with and without the clips to isolate the specific impact of these clips on ablation outcomes (Fig. 5 A–C). The presence of metallic clips resulted in a reduction of electric field strength in their immediate surrounding microscopic volume, with maximum distortion at the middle of the clip, along the longitudinal axis. The reduction in electric field strength at the site of such distortions was sufficient to reduce the efficacy of cell death (Fig. 5D). Such distortions in the electric field strength were restricted to < 1mm away from the clip, (Fig. 5E,F) and no difference was found in gross volume of tumor experiencing electric field at the critical threshold when comparing simulations performed with, and without the clips (p=0.8852, Table 4).

Correlation of Simulation – Clinical Outcomes

Based on computed electric field coverage and cell death probaility, simulation results from patient specific models correlated with clinical outcomes, predicting LTP in all patients with metallic surgical clips (Fig. 2E, 3D, 5D). Two patients without clips, and all four patients having clips were seen to have inadequate electric field coverage in the tumor and the margin, however, having cell death in > 95 % of tumor volume seemed to improve local tumor control in patients without clips. Overall, there was no statistically significant difference in the percentage volume of the tumor experiencing electric field coverage greater than the critical threshold (MI: 78.2 ± 16% vs no MI: 91.6 ± 8.8%, p = 0.3123) or the estimated probability of cell death within the ablation (MI: 81.4 ± 18.7% vs no MI: 96.5 ± 1.9%, p = 0.1939) between the two patient groups, with the presence of clips being the only differentiating factor.

Risk of thermal damage from MI.

Due to the large number of pulses delivered during IRE treatment, thermal damage could be observed in a significant volume of target tissue. However, the percentage volume of the tumor where cell kill was expected due to thermal damage was completely enclosed within the volume of cell death from IRE. (Fig. 6A–D). In patients having clips, simulations performed with (60.9 ± 18.1%) and without the clips (60.8 ± 18.2%, p = 0.8852) did not reveal a difference in the degree of thermal damage, stemming from the presence of metal in the treatment region. Likewise, there was no difference in the volume of thermal damage within the ablation between the two patient cohorts (p = 0.8852).

Discussion

CRLM often presents as infiltrative disease, with high risk of recurrence at the surgical margin in patients having unfavorable mutational status (18,19). Anatomic location of the surgical margin can influence choice of loco-regional treatment to manage recurrent disease. IRE has emerged as potential choice for the management of these patients as the technique can be safely applied in delicate anatomic locations even if the tumor involves critical structures (2,6,7,30). Tumor size has been previously identified as an predictor of LTP in

IRE (3), which was confirmed in our analysis as well. Our results suggest that IRE requires further optimization and refinement when treating CRLM, especially when the treatment site has MI such as surgical clips. As evidenced by our experience, application of IRE without adjusting treatment parameters to account for the presence of metallic surgical clips reduces treatment efficacy.

IRE in patients using the Nanoknife system is contraindicated in the presence of large MI such as stents as per the manufacturer's instruction for use. However, the impact of smaller MI such as surgical clips was largely considered negligible. Our simulation results suggest that the presence of MI in tissue being treated with IRE can distort both the electrical and thermal field distribution, resulting in an unpredictable ablation zone. This consideration has resulted in multiple preclinical studies evaluating the safety and impact of the presence of metallic implants on IRE treatment. Using a tuber model, Neal et al. (20) evaluated the impact of metallic seeds on electric field distribution and the ablation volume, reporting no deleterious effects. However, in vivo preclinical evaluation by Ben-David et al. (9) has shown the presence of metal in the IRE treatment zone can distort the size and shape of the ablation. Scheffer et al. (8), and Dunki-Jacobs et al. (21) have then shown that IRE can cause localized heating, with the presence of metal increasing thermal damage at the treatment site. In a case report, Mansson et al. (22) present contraindication to the use of IRE in patients who have bare metal stents from the elevated risk of severe adverse events. We add to these prior results by reporting that the presence of metallic surgical clips can impact the efficacy of IRE when treating CRLM in a clinical setting but does not seem to impact ablation safety.

Ablation with IRE is amenable to numerical modeling, which has been validated in multiple preclinical and clinical studies as a tool for predicting the safety and efficacy of this technique (12–14,23–25). However, the use of simulation tools for treatment planning for IRE is not standard of care and is not performed in current clinical practice. In this study we employ patient specific numerical models as a tool to understand the etiology and factors underlying IRE failure when used to treat CRLM patients having metallic surgical clips at the site of ablation. We observed that metallic clips induce microscopic distortions in the electric field used to perform IRE while having negligible effect on the overall volume of tissue experiencing electric field strength above the critical threshold. We also found that the electric field coverage was often inadequate for the tumor and its margin irrespective of the metallic clip's presence, which may explain tumor recurrence away from the location of MI in some patients. Despite inadequate coverage, LTP was not observed in patients without clips possibly because of higher estimated cell kill probability. The cell death probability calculations takes into account the number of pulses delivered into a tissue and increased pulse numbers seems to improve tumor control even in regions of reduced electric field strength which is consistent with theory (26,27). Ablation with IRE involves interplay between different treatment parameters (voltage, pulse duration, and the number of pulses applied) and IRE planning based only on electric field coverage may therefore be inadequate to ensure successful treatment. Our experimental findings suggest incorporation of simulation for planning can assist in appropriate probe placement and optimization of electrode geometry prior to pulse delivery. Appropriate electrode orientation with respect to

the metallic implant may reduce distortions in the electric field, thereby minimizing the impact of MI on ablation outcomes.

While increasing pulse application has been seen as a way to increase the efficacy of IRE, any benefit from increased pulse application has to be carefully considered in light of associated thermal damage during IRE consistent with previous calculations and recent ex vivo experiments (16,28). While IRE has a predominantly non-thermal cell kill mechanism (29), all our simulations suggested the existence of thermal damage in a considerable volume of the treated tissue. Since metal is a good thermal and electrical conductor, the presence of metallic implants at the treatment site does not result in their direct heating but increases the thermal energy deposited into the tissue surrounding the implant. Such localized heating can reduce the safety associated with IRE (8,21), which often is the motivating rationale when selecting this treatment technique for use in specific clinical conditions. Precise treatment planning, with use of patient-specific simulation models prior to treatment delivery can improve electrode positioning and treatment parameter selection to improve treatment outcomes even in patients having metallic implants at the treatment site.

Our study is limited by its retrospective nature and the small number of patients included. Likewise, the patient specific simulation models were performed only in a subset of all patients that were treated at our center, potentially limiting the generalizability of our findings. Expanding the data with additional patients and simulation models can increase our knowledge of IRE for the treatment of CRLM, which will be the focus of future studies. As a retrospective study, with an inherent patient selection bias, we are unable to control for the volume or number of metallic implants in the ablation or evaluate the effect in different types of clips based on material (stainless steel vs. titanium).

In conclusion, the presence of metallic surgical clips within 1 cm from the tumor margin is associated with increased risk of treatment failure after IRE of CRLM, but safety is not affected. Potentially, increasing pulse application can offset electric field distortion in the presence of metallic implants, but this may reduce the non-thermal benefits of IRE. The results of this study emphasize the importance of an adequate patients' selection and a detailed treatment planning process, which could help to reduce the tumor recurrences while avoiding complications after percutaneous IRE of CLRM.

Acknowledgements:

Funding: The authors acknowledge the support of NIH Cancer Center Support Grant (P30 CA008748) for core laboratory services that were used for the presented work. The authors acknowledge the support of the National Cancer Institute of the National Institutes of Health under Award Number U54CA137788/U54CA132378, and the Slovenian Research Agency (ARRS), Slovenia Program P2-0249, Grant Z3-7126 and Bilateral Slovenian-USA project BI-US/18-19-002.

References

1. Kingham TP, Karkar AM, D'Angelica MI, et al. Ablation of Perivascular Hepatic Malignant Tumors with Irreversible Electroporation. Journal of the American College of Surgeons. 2012;215(3):379–387. [PubMed: 22704820]

2. Cannon R, Ellis S, Hayes D, Narayanan G, Martin RCG. Safety and early efficacy of irreversible electroporation for hepatic tumors in proximity to vital structures. J Surg Oncol. 2013;107(5):544–549. [PubMed: 23090720]

3. Niessen C, Igl J, Pregler B, et al. Factors Associated with Short-Term Local Recurrence of Liver Cancer after Percutaneous Ablation Using Irreversible Electroporation: A Prospective Single-Center Study. Journal of Vascular and Interventional Radiology. 2015;26(5):694–702. [PubMed: 25812712]

4. Scheffer HJ, Nielsen K, van Tilborg A a JM, et al. Ablation of colorectal liver metastases by irreversible electroporation: results of the COLDFIRE-I ablate-and-resect study. Eur Radiol. 2014;24(10):2467–2475. [PubMed: 24939670]

5. Schoellhammer HF, Goldner B, Merchant SJ, Kessler J, Fong Y, Gagandeep S. Colorectal liver metastases: making the unresectable resectable using irreversible electroporation for microscopic positive margins – a case report. BMC Cancer. 2015;15(1):271. [PubMed: 25886376]

6. Dollinger M, Zeman F, Niessen C, et al. Bile Duct Injury after Irreversible Electroporation of Hepatic Malignancies: Evaluation of MR Imaging Findings and Laboratory Values. J Vase Interv Radiol. 2016;27(1):96–103.

7. Silk MT, Wimmer T, Lee KS, et al. Percutaneous ablation of peribiliary tumors with irreversible electroporation. J Vase Interv Radiol. 2014;25(1):112–118.

8. Scheffer HJ, Vogel JA, van den Bos W, et al. The Influence of a Metal Stent on the Distribution of Thermal Energy during Irreversible Electroporation. PLoS ONE. 2016;ll(2):e0148457.

9. Ben-David E, Ahmed M, Faroja M, et al. Irreversible electroporation: treatment effect is susceptible to local environment and tissue properties. Radiology. 2013;269(3):738–747. [PubMed: 23847254]

10. Goldberg SN, Grassi CJ, Cardella JF, et al. Image-guided Tumor Ablation: Standardization of Terminology and Reporting Criteria. Radiology. 2005;235(3):728–739. [PubMed: 15845798]

11. Ahmed M, Solbiati L, Brace CL, et al. Image-guided tumor ablation: standardization of terminology and reporting criteria-a 10-year update. Radiology. 2014;273(l):241–260. [PubMed: 24927329]

12. Marčan M, Pavliha D, Kos B, Forjanič T, Miklavčič D. Web-based tool for visualization of electric field distribution in deep-seated body structures and planning of electroporation-based treatments. Biomed Eng Online. 2015;14 Suppl 3:S4.

13. Kos B, Voigt P, Miklavcic D, Moche M. Careful treatment planning enables safe ablation of liver tumors adjacent to major blood vessels by percutaneous irreversible electroporation (IRE). Radiol Oncol. 2015;49(3):234–241. [PubMed: 26401128]

14. Garcia PA, Kos B, Rossmeisl JH, Pavliha D, Miklavčič D, Davalos RV. Predictive therapeutic planning for irreversible electroporation treatment of spontaneous malignant glioma. Med Phys. 2017;44(9):4968–4980. [PubMed: 28594449]

15. Dermol J, Miklavčič D. Mathematical Models Describing Chinese Hamster Ovary Cell Death Due to Electroporation In Vitro. J Membr Biol. 2015;248(5):865–881. [PubMed: 26223863]

16. Garcia PA, Davalos RV, Miklavcic D. A numerical investigation of the electric and thermal cell kill distributions in electroporation-based therapies in tissue. PLoS ONE. 2014;9(8):el03083.

17. Donoghoe MW, Gebski V. The importance of censoring in competing risks analysis of the subdistribution hazard. BMC Medical Research Methodology. 2017;17(1):52. [PubMed: 28376736]

18. Margonis GA, Sasaki K, Andreatos N, et al. KRAS Mutation Status Dictates Optimal Surgical Margin Width in Patients Undergoing Resection of Colorectal Liver Metastases. Ann Surg Oncol. 2017;24(1):264–271. [PubMed: 27696170]

19. Akyuz M, Aucejo F, Quintini C, Miller C, Fung J, Berber E. Factors affecting surgical margin recurrence after hepatectomy for colorectal liver metastases. Gland Surg. 2016;5(3):263–269. [PubMed: 27294032]

20. Neal RE, Smith RL, Kavnoudias H, et al. The effects of metallic implants on electroporation therapies: feasibility of irreversible electroporation for brachytherapy salvage. Cardiovasc Intervent Radiol. 2013;36(6):1638–1645. [PubMed: 23942593]

21. Dunki-Jacobs EM, Philips P, Martin RCG. Evaluation of thermal injury to liver, pancreas and kidney during irreversible electroporation in an in vivo experimental model. Br J Surg. 2014;101(9):1113–1121. [PubMed: 24961953]

22. Månsson C, Nilsson A, Karlson B-M. Severe complications with irreversible electroporation of the pancreas in the presence of a metallic stent: a warning of a procedure that never should be performed. Acta Radiol Short Rep. 2014;3(11):2047981614556409.

23. Edhemović I, Brecelj E, Gasljevic G, et al. Intraoperative electrochemotherapy of colorectal liver metastases. J Surg Oncol. 2014;110(3):320–327. [PubMed: 24782355]

24. Edhemovic I, Gadzijev EM, Brecelj E, et al. Electrochemotherapy: a new technological approach in treatment of metastases in the liver. Technol Cancer Res Treat. 2011;10(5):475–485. [PubMed: 21895032]

25. Djokic M, Cemazar M, Popovic P, et al. Electrochemotherapy as treatment option for hepatocellular carcinoma, a prospective pilot study. Eur J Surg Oncol. 2018;44(5):651–657. [PubMed: 29402556]

26. Rems L, Miklavčič D. Tutorial: Electroporation of cells in complex materials and tissue. Journal of Applied Physics. 2016;119(20):201101.

27. Yarmush ML, Golberg A, Serša G, Kotnik T, Miklavčič D. Electroporation-based technologies for medicine: principles, applications, and challenges. Annu Rev Biomed Eng. 2014;16:295–320. [PubMed: 24905876]

28. O'Brien TJ, Bonakdar M, Bhonsle S, et al. Effects of internal electrode cooling on irreversible electroporation using a perfused organ model. Int J Hyperthermia. 2018;1–12.

29. Faroja M, Ahmed M, Appelbaum L, et al. Irreversible electroporation ablation: is all the damage nonthermal? Radiology. 2013;266(2):462–470. [PubMed: 23169795]

30. Vroomen LGPH, Petre EN, Cornells FH, Solomon SB, Srimathveeravalli G. Irreversible electroporation and thermal ablation of tumors in the liver, lung, kidney and bone: What are the differences? Diagn Interv Imaging. 2017 9;98(9):609–617. [PubMed: 28869200]

31. Gallinato O, de Senneville BD, Seror O, and Poignard C. Numerical workflow of irreversible electroporation for deep-seated tumor. Phys. Med. Biol, vol. 64, no. 5, p. 055016, 3 2019. [PubMed: 30669121]

32. Filippiadis DK, Binkert C, Pellerin O, Hoffmann RT, Krajina A, Pereira PL. CIRSE Quality Assurance Document and Standards for Classification of Complications: The CIRSE Classfication System. Cardiovasc Intervent Radiol. 2017 8; 40(8) 1141–1146. [PubMed: 28584945]

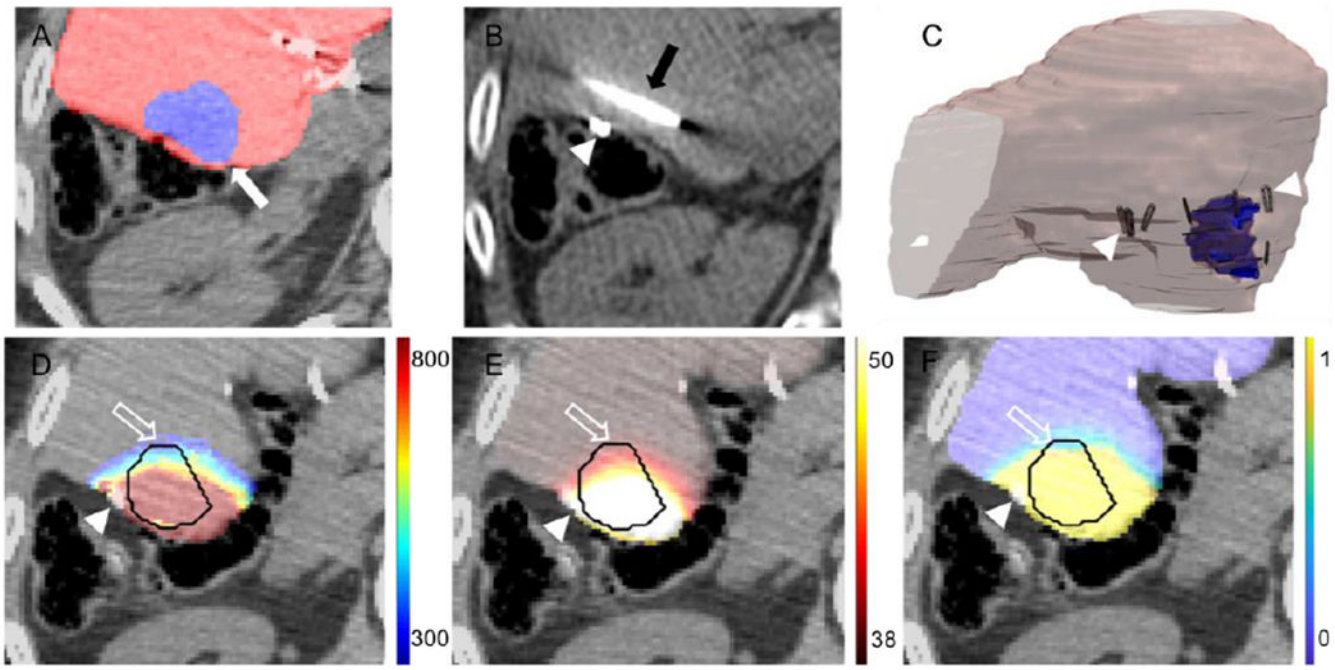

Figure 1.

Workflow of patient specific simulation models. A. Pre-treatment CT images were segmented to extract the tumor (white arrow) and surrounding parenchyma. B. Intra-treatment CT imaging is used to identify the location of clips (arrowhead) and ablation probes (black arrow). C. The segmented images are converted to 3D models, arrowheads indicate location of surgical clips relative to the tumor (outlined in blue). Calculation of D. electric field distribution (units in V/cm), E. thermal damage (units degree centigrade) and F. cell kill probability (fraction 0-1) in the tumor and margin (outline arrow). The tumor is outlined in black, axial cross sections selected to show the tumor at the largest cross section and the relative location of the surgical clips (arrowhead).

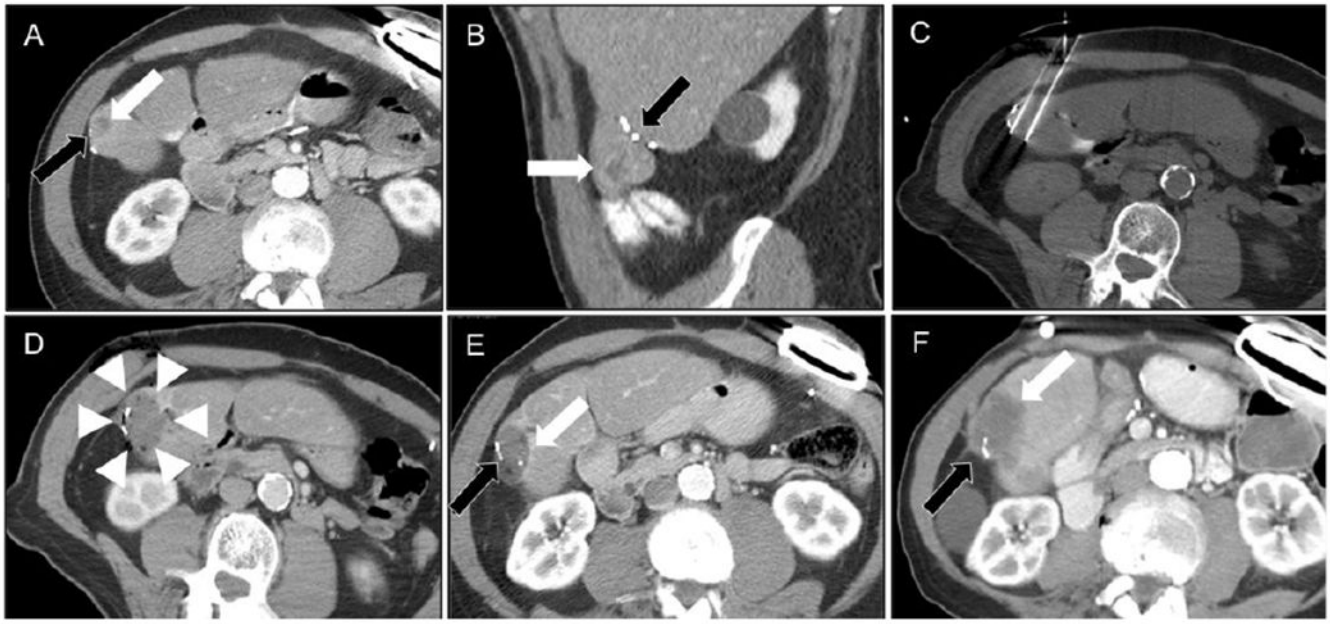

Figure 2:

Example of CRLM treated with IRE in patient number two who had surgical clips in the treatment region. A and B. Pre-treatment CT image showing tumor location (white arrow) and relative location of the surgical clips (black arrow). C. Intra-treatment CT image showing ablation probe placement. D. Immediate post-IRE image showing technical treatment success (arrowheads). Tumor recurrence (white arrow) on CECT at E. 8 and F. 24 months following IRE, abutting the metallic implant (black arrow).

Figure 3:

Example of CRLM treated with IRE in patient number one who had surgical clips in the treatment region. A. Pre-treatment CT image showing tumor location (white arrow) and the relative location of the surgical clips (black arrow). Local tumor progression (white arrow) assessed with B. CT imaging and C. PET imaging at 12 months post-IRE.

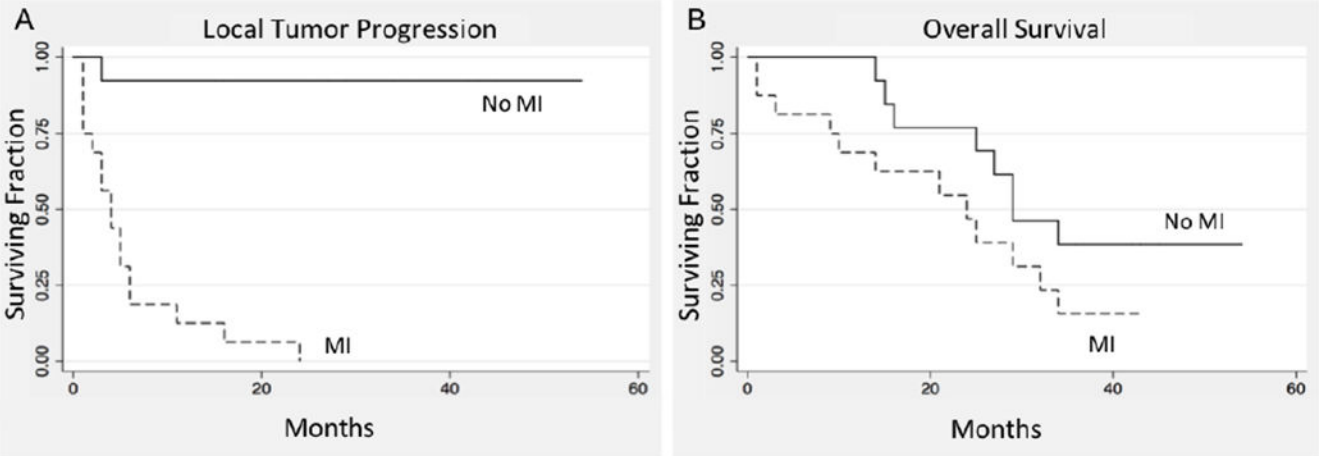

Figure 4.

Kaplan Meier estimate of A. local tumor progression free survival (HR=29.5, [3.5-47.2], p=0.002) and B. overall survival (HR=2; [0.81-4,92]; p=0.132). after IRE with or without presence of metallic implants within 1 cm from the tumor margin.

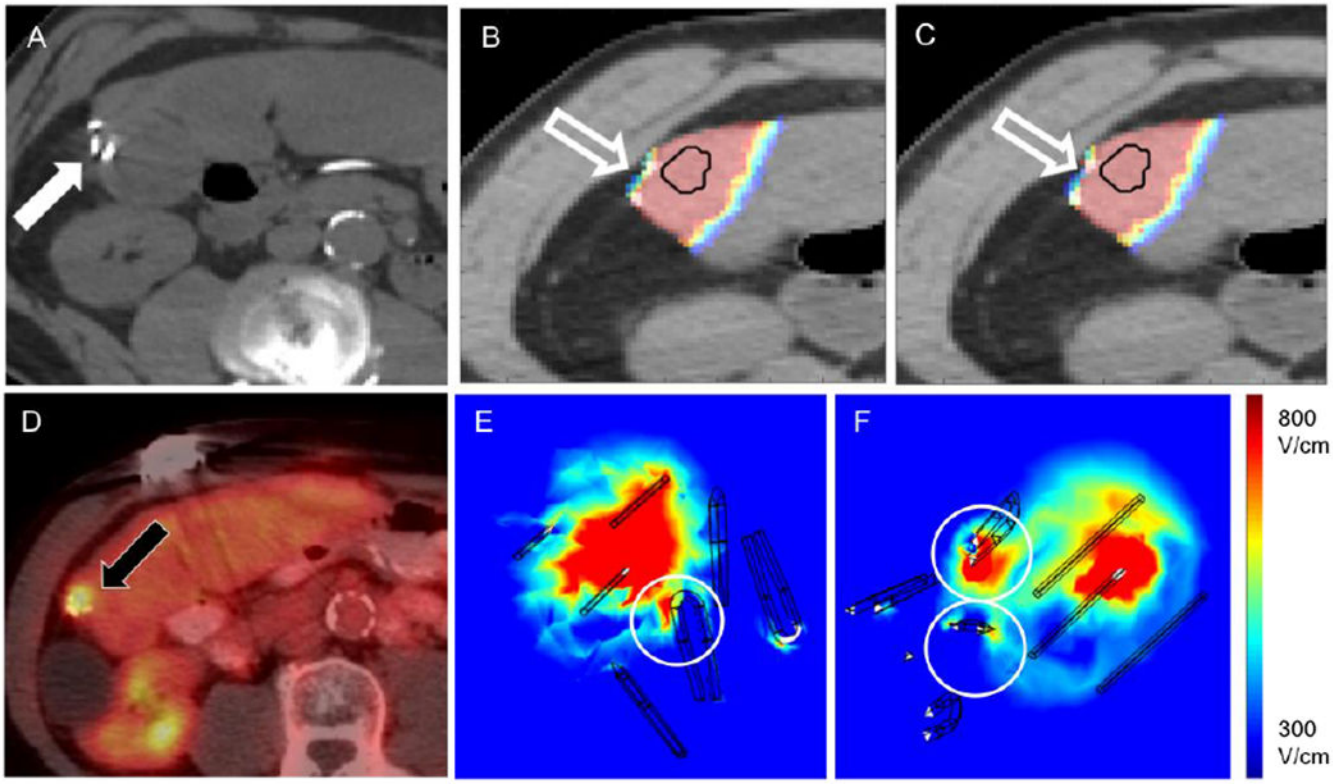

Figure 5.

Simulation model constructed for patient number two. A. Pre-IRE image showing the location of surgical clips within the treatment region (white arrow). Estimate of electric field coverage when simulations were performed B. without or C. with the surgical clips (outline arrows). D. Local tumor progression observed on PET margin. imaging at 24 months post-IRE (black arrow). E,F. Computed electric field distribution in target tissue, distortions are visible in the vicinity of the clips (circles).

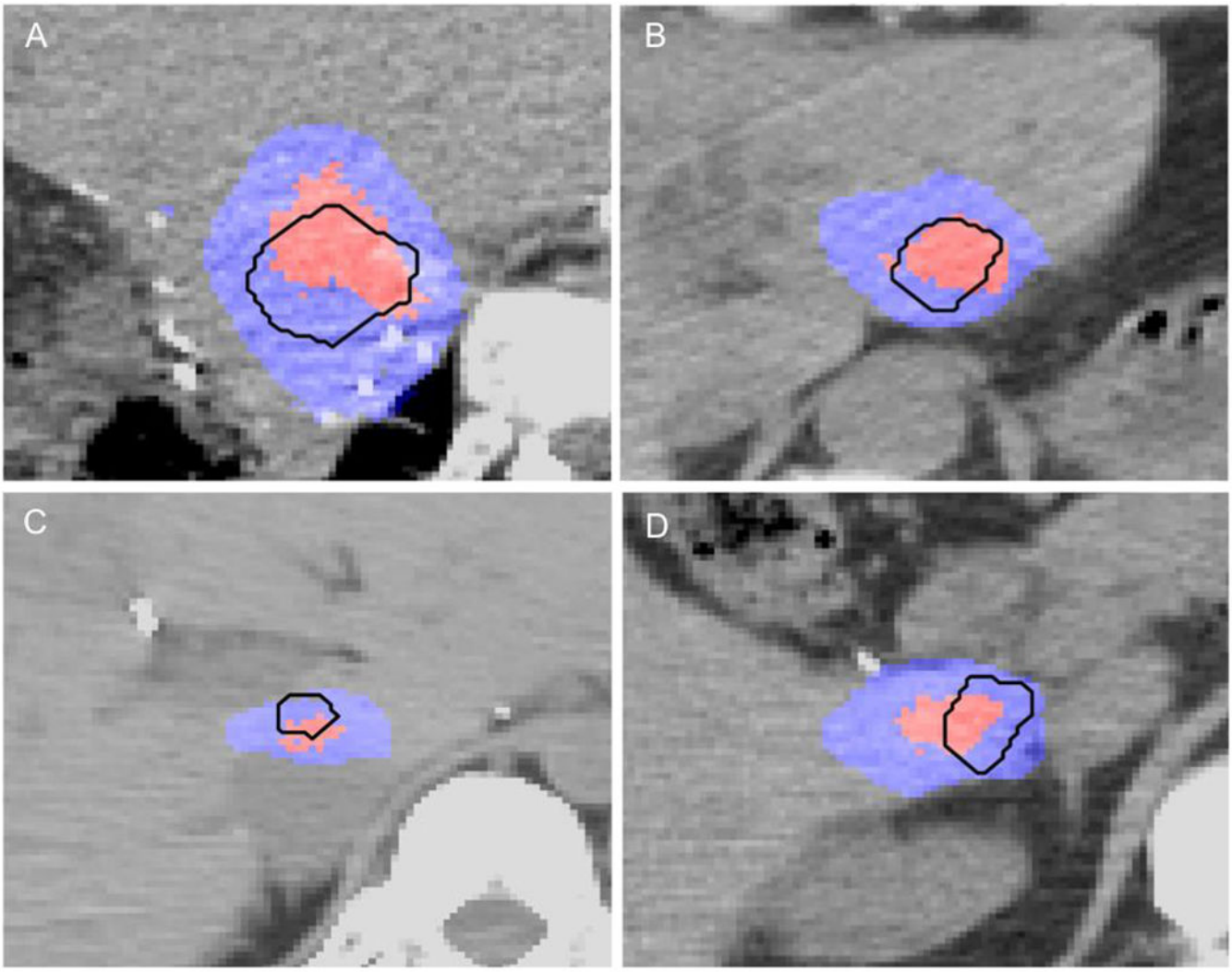

Figure 6.

Volume of thermal damage during IRE in A. Patient number four, B. Patient number five, C. Patient number six and D. Patient number seven. The tumor is outlined in black, the region of thermal damage is depicted in red and the total region of IRE is shown in blue. Tissue was considered ablated (thermally or by IRE) if cell kill probability was above 0.9.

Table 1:

Patient and Tumor Characteristics

Characteristics	MI	No-MI
No. of patients	13	12
No. of lesions	17	12
Age (years)	51.7 ± 10.7	61 ± 12.7
Sex	7 male / 6 female	6 male / 6 female
Tumor size (cm)	2.80 ± 0.76	1.45 ± 0.78

Note: Data are expressed as mean values ± standard deviation.

Table 2:

Treatment characteristics, recorded from the IRE generator

No. of probes	3 (2-6)
Probe spacing (mm)	15 (10 - 25)
Treatment voltage (V)	1890 (1050 – 3000)
Num. pulses per probe	90 (70 – 90)
Pulse width (uS)	90 (90 – 100)
Impedance change (ohms)	−13.5 (−3.7 – −38.5)
Peak current (A)	27.5 (8.9 – 50)
Cumulative energy delivered (J)	406.8 (74.5 – 938.2)

Note.— Data are expressed as median values ± standard deviation, and range is given in parenthesis.

Table 3:

Univariate and Multivariate Analyses of Factors Associated with Local Tumor Progression by Using Regression Models

	Univariate Analysis	Multivariate Analysis		
	P value	**HR**	**CI95%**	***P value***
Size(>2 cm)	*0.003*	1.65	0.6-4.9	*0.364*
Distance of probes (> 20 mm)	*0.018*	0.99	0.3-3.5	*0.996*
Metallic implants	*0.001*	29.5	3.5-247.2	*0.002*

Note.—All examined variables displayed significance at univariate analysis and multivariate analysis. Multivariate analysis data were calculated with the regression model.

Table 4:

Electric field coverage and cell kill probability in tumor volume

Patient #	Electric field coverage* (%)		IRE cell kill** (%)		Thermal cell kill*** (%)	
	no clips	clips	no clips	clips	no clips	clips
1	94.57	94.63	93.61	93.87	86.74	86.68
2	59.32	58.94	55.70	55.51	51.90	52.09
3	71.26	71.18	79.53	81.03	59.34	59.84
4	87.98	87.35	96.89	96.53	45.66	44.75
5	98.71	/	95.76	/	68.63	/
6	87.04	/	95.37	/	35.19	/
7	81.44	/	95.62	/	29.90	/
8	99.48	/	99.48	/	90.63	/

Note. —

*Percentage of tumor volume covered with electric field of at least 500 V/cm.

**Percentage of tumor volume with cell death probability above 0.9 due to irreversible electroporation alone (Peleg-Fermi model adapted from (15)).

***Percentage of tumor volume with cell death probability above 0.9 due to thermal damage alone.